The PY4 Mission: A Low-Cost Demonstration of CubeSat Formation-Flying Technologies

Max Holliday, Rachel Ticknor
Axient/MEIS (at NASA Ames Research Center)
max.a.holliday@nasa.gov, rachel.l.ticknor@nasa.gov

Jan Stupl, Roger Hunter
NASA Ames Research Center
jan.stupl@nasa.gov, roger.c.hunter@nasa.gov

Paulo Fisch, Ibrahima Sory Sow, Jacob Willis, Zachary Manchester
Carnegie Mellon University
pfisch@cmu.edu, isow@andrew.cmu.edu, jwillis2@andrew.cmu.edu, zacm@cmu.edu

ABSTRACT

The PY4 mission aims to enable autonomous swarms of small spacecraft by both reducing the manufacturing cost and integration effort required for individual spacecraft, and by advancing guidance, navigation, and control algorithms that increase autonomy and reduce or eliminate the need for expensive sensor, actuator, and propulsion hardware. PY4 consists of four 1.5U CubeSats, and builds on the PyCubed open-source avionics platform and the previous V-R3x mission. To date, PY4 has successfully demonstrated high-data-rate mesh networking, precise inter-satellite ranging, range-based relative orbit determination, and magnetorquer-only sun pointing. A drag-based formation-flying experiment is also planned for an extended mission.

INTRODUCTION

The advent of CubeSats and availability of low-cost commercial ride-share services have increased interest in missions involving formations or swarms of multiple spacecraft. Such mission concepts offer the promise of continuous coverage of the Earth for observation and communication services [1]–[3], large baselines for high-resolution radio and optical astronomy [4], [5], and distributed in-situ measurements of the ionosphere and solar wind [6], [7]. However, current methods for performing the basic relative-navigation and formation-flying functions required for multi-spacecraft swarms involve expensive, specialized hardware; highly centralized coordination and control, typically performed by ground operators; and limited ability to function beyond low-Earth orbit due to reliance on GPS or other Global Navigation Satellite System (GNSS) signals.

The PY4 mission aims to demonstrate low-cost sensing, communication, and navigation capabilities to enable scalable, autonomous CubeSat swarms. This includes building on a highly integrated open-source avionics stack that relies on commercial off-the-shelf (COTS) electronic components to reduce manufacturing costs, and developing novel navigation algorithms that can be implemented in flight software onboard compute-constrained CubeSats. PY4 is led by Carnegie Mellon University and funded by the NASA Small Satellite Technology Program. NASA Ames provided support for integration and testing. PY4 builds on the open-source PyCubed avionics and software platform [8] and the previous V-R3x mission [9].

PY4 makes use of COTS LoRa radio modules that perform both communication and two-way time-of-flight ranging between spacecraft [10]. These range measurements are fused with orbital dynamics models and other navigation measurements — such as occasional GPS measurements from a single “anchor” satellite — to determine the full orbital parameters of the entire swarm.

The four PY4 spacecraft launched on the SpaceX Transporter 10 mission on March 4, 2024. So far, they have successfully achieved baseline mission requirements, including demonstrating precise inter-satellite ranging, relative orbit determination, and magnetorquer-only sun pointing. A planned extended mission will also demonstrate drag-based formation-flying. Taken together, these capabilities enable swarms of low-cost spacecraft that can control their attitude and formation fly without relying on large, costly, and failure prone reaction wheels or propulsion systems.

The paper proceeds as follows: Section 2 provides an overview of the PY4 mission concept, followed by a discussion of the spacecraft’s hardware, electronic, and software design in Section 3. Sections 4, 5, and 6 then summarize the attitude control, relative navigation, and drag-based formation-flying capabilities of PY4, respectively. Section 7 provides on-orbit experimental results validating sun-pointing and range-based relative

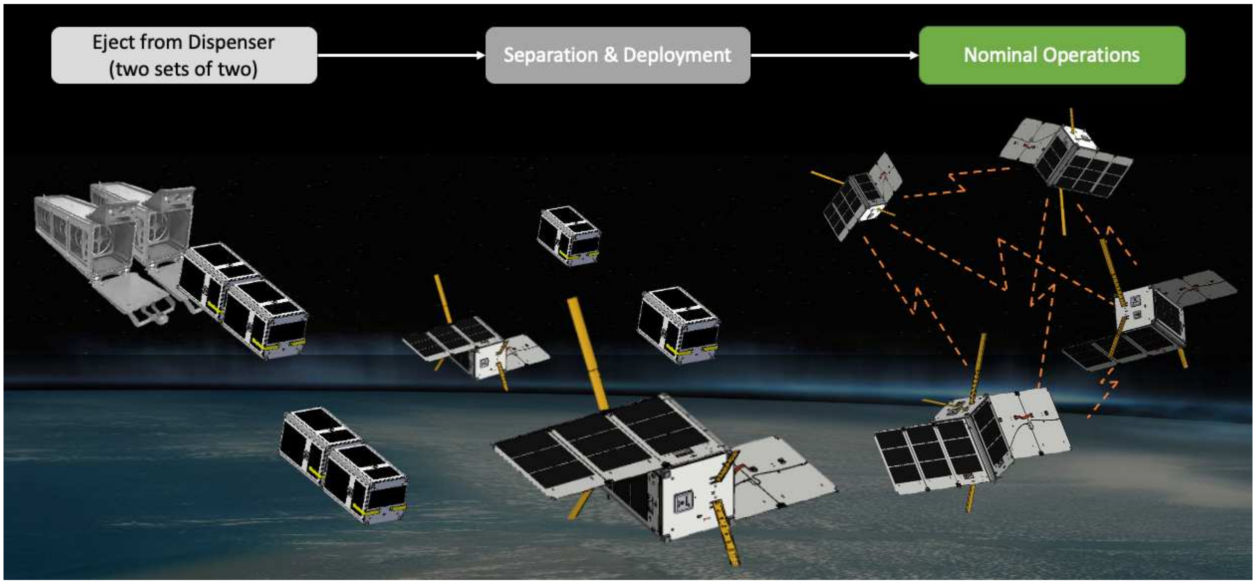

Figure 1: PY4 mission timeline. From left to right: Four spacecraft are ejected in pairs from two dispensers. Deployment timing is optimized to minimize satellite dispersion while still ensuring low collision risk. Next, spacecraft deploy antennas and solar panels.

navigation algorithms. Finally, Section 8 summarizes our conclusions and directions for future work.

MISSION CONCEPT

The PY4 mission is designed to demonstrate coordination of multiple low-cost CubeSats via radio cross linking, mesh networking, and range-based relative navigation. The mission includes four 1.5U CubeSats deployed into an initial 515 km altitude circular sun-synchronous orbit. A summary of spacecraft operations is illustrated in Fig. 1.

The four 1.5U PY4 spacecraft are deployed in pairs from a Nanosatellite Launch Adapter System (NLAS) 6U deployer provided by launch integrator Maverick Space Systems, and are expected to exit their dispensers in a slow tumble with small initial relative velocities. Since they do not have propulsion systems, the spacecraft will drift apart over time due to their initial relative velocities and the integrated effects of differential drag. The delay between deployment of the two pairs was carefully optimized to minimize satellite dispersion while still ensuring low collision risk. Monte-Carlo simulations over a range of different possible atmospheric conditions and realistic deployment delta-V bound the drift between spacecraft at a few kilometers per hour. The spacecraft are expected to drift out of range of each other's radios a few weeks after deployment.

Relative Navigation

To ensure that networking and ranging between all four spacecraft can be accomplished at a variety of different distance scales, the spacecraft deploy their antennas and solar panels and then begin transmitting within seconds of their deployment from the dispensers. All data is logged in non-volatile memory onboard the spacecraft to be downlinked later. The spacecraft are programmed to perform ranging experiments every 60 seconds for the duration of the mission. Alternatively, commands can also be uplinked to stop ranging operations if it is deemed that sufficient data has been collected.

Simultaneously with ranging and networking experiments, the four PY4 spacecraft will also collect GPS position and velocity data to provide precision timestamps for all experimental data and to provide ground-truth positions to validate inter-satellite range measurements. Since individual GPS measurements are less accurate than the range measurements collected by the spacecrafts' LoRa radios, GPS time-series data will be smoothed in post-processing using standard Kalman smoother techniques to produce more accurate position estimates.

In addition to simply validating the accuracy of LoRa ranging, the inter-satellite range data will also be used to compute full spacecraft position and velocity estimates. Since full, unambiguous orbit determination is, in general, not possible using only inter-satellite ranging [11], one spacecraft will be treated as an "anchor node," and will be assumed to have full orbit knowledge from its GPS receiver. The orbits of the other three spacecraft will then be determined using only range data to the anchor node. The designation of anchor is arbitrary.

Coordinated Radiation Measurements

Simultaneously with ranging and networking experiments, the four PY4 spacecraft will also collect total-ionizing dose (TID) radiation measurements once every 30 seconds with the intent of creating dense temporal and spatial dose-rate datasets. Custom dosimeters that will be used to collect this TID information are comprised of the threshold voltage (V_{TH}) direct-readout circuit described in [12] for monitoring V_{TH} in a commercial P-channel MOSFET (Vardis VT101) designed for dosimetry with known TID response characteristics.

Attitude Control

After completion of ranging operations, commands are uplinked to the spacecraft to detumble and perform a sun-pointing demonstration using a novel magnetorquer-only “safe-mode” attitude stabilization controller. The spacecraft will spin about their major axis of inertia at approximately 20 deg/s and orient their spin axis such that their large solar panels are facing the sun. This attitude configuration is passively stable, so that the spacecraft will remain sun-pointed even if the controller is turned off. It also has the advantage of requiring only very reliable low-cost sensor and actuator hardware.

Table 1: PY4 Primary Mission Requirements

Requirement	Description
S-Band Ranging	PY4 shall demonstrate ranging with 1 m precision at a distance of at least 10 km between at least two satellite nodes.
Distributed Sensor Collection	PY4 shall coordinate and collect at least one radiation data packet from on-board sensors from each satellite node.
Relative Position Determination	PY4 shall demonstrate on-orbit range-only relative positioning between all satellite nodes to an accuracy of 100 m (1-sigma).
OTA Software Updates	PY4 shall perform an over-the-air software update on at least one satellite node with autonomous updates to at least one other node.
Magnetorquer-Only Sun Pointing	PY4 shall demonstrate 3-axis magnetorquer-only sun pointing on at least one satellite node to an accuracy of 10 deg (1-sigma).

Primary Mission

The PY4 primary mission requirements are summarized in Table 1. Once data collection for these primary objectives is complete – likely within the first two weeks of the mission depending on the drift rates between the spacecraft – all of the data stored on the four spacecraft will be downlinked opportunistically to ground stations. All four PY4 spacecraft transmit a beacon message every 30 seconds using their 915 MHz UHF LoRa radios. Each beacon is a single packet with a 60-byte payload containing state-of-health information, mission status, and a revolving summary of telemetry and experiment data. Additionally, a single command can place one of the spacecraft into data downlink mode, at which point all stored experimental data is transmitted at a high rate by the UHF LoRa radio.

Extended Mission

The PY4 extended mission requirements are summarized in Table 2. During an extended mission, after all primary mission objectives are completed, several additional demonstrations will be pursued. The most ambitious of these is a drag-based formation-flying demonstration in which a magnetorquer-based attitude control system will be used to maintain spacecraft in a high- or low-drag state to alter their orbits. The goal will be to maintain spacecraft in close enough proximity to maintain radio crosslinks and prevent their orbital positions from drifting apart.

Table 2: PY4 Extended Mission Requirements

Requirement	Description
OTA Firmware Update	PY4 shall perform at least one successful over-the-air firmware update from at least one satellite node.
Drag-Based Formation Flying	PY4 shall demonstrate drag-based formation flying, keeping at least two spacecraft within 100 km of each other for a minimum of 24 hours.
Distributed Absolute Position Determination	PY4 shall demonstrate on-orbit absolute positioning between all satellite nodes using ranges from all satellite nodes and a single node with GPS to an accuracy of 100 m (1-sigma).
SDR-Based GPS	PY4 shall demonstrate acquisition of at least one GPS lock from an SDR from at least one satellite node.

SPACECRAFT DESIGN

The PY4 spacecraft were developed with minimizing hardware cost and development time as primary drivers. All aspects of the spacecraft were developed in house by a small team from conception to launch in 14 months, including:

- Avionics: power handling, energy harvesting, data processing and data storage
- Flight software: low-level firmware, mesh networking, S-band ranging, communication, and over-the-air updating
- Mechanical design: deployable antennas and solar arrays
- Flight hardware fabrication, assembly, and testing

This extremely fast development time was enabled by the use of open-source avionics and software from the

PyCubed project [8], which has been developed by several of the and used on previous CubeSat missions, including KickSat-2 [13] and V-R3x [9]. The four PY4 flight units are shown in Fig. 2, and a cutaway illustration depicting the major components of the 1.5U PY4 CubeSat is shown in Fig. 3. The major subsystems of the spacecraft are detailed in the following subsections.

Figure 2: Four 1.5U PY4 spacecraft flight units.

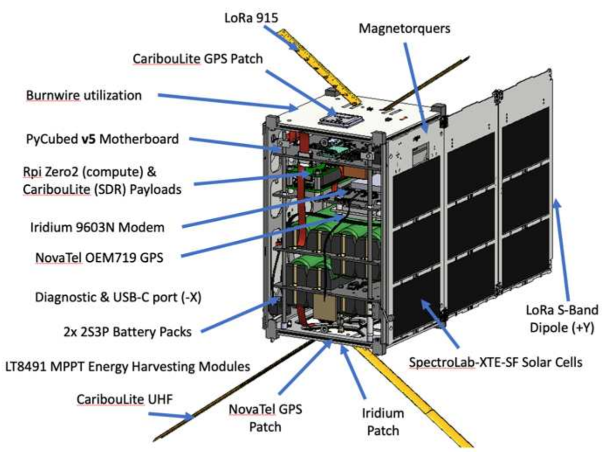

Figure 3: Cutaway view of the PY4 spacecraft.

Mechanical

PY4 is bult to conform to the 1.5U CubeSat specification. Each spacecraft's mass is approximately 2 kg. The spacecraft structures are standard 1.5U anodized aluminum chassis from Pumpkin, Inc. with minor modifications to accommodate antenna, solar panel, and deployment switch mounting. The UHF dipole antennas are made from steel spring tape and are designed to be folded against the exterior faces of the CubeSat when mounted in the dispenser. Burn wires are used to deploy both sets of dipole antennas and both deployable solar arrays. The full set of components used in a single PY4 flight build are shown in Fig. 4.

The decision to add deployable solar panels was made near the end of the development process. Risk of this late-stage design addition was reduced by making the panels entirely optional from an electrical and mechanical perspective. Thorough prototyping, testing, and dispenser fit checks were performed before the deployable panels were finalized for the flight design.

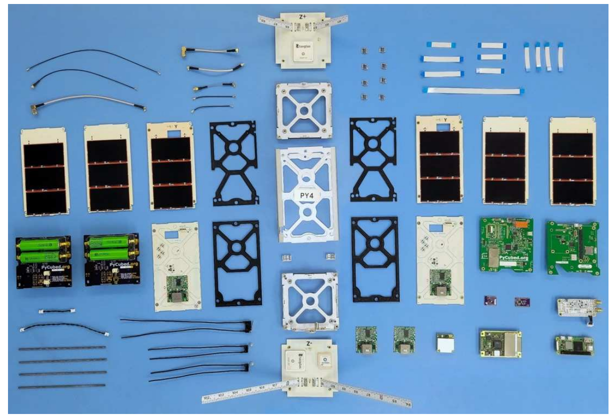

Figure 4: All components of a single PY4 spacecraft before final assembly.

Suitable hinge designs that could lock into place and fit the mission's size requirements could not be found. Therefore, a simple low-cost hinge was developed and tested (Fig. 5). The intent was to develop a hinge that was small enough to minimize impact on solar-cell placement and allow two additional 1.5U panels per Y face to fit within the allowable dispenser volume. Additionally, the hinge design aims to be low cost and cheap to manufacture. The resulting 32 sets of flight hinges met the needs of the mission but proved to be more labor intensive to fabricate than intended. For future use, it is recommended that additional design-for-manufacturing iterations be performed to reduce the necessary labor and improve uniformity across sets.

Figure 5: Solar panel hinge in deployed and locked configuration.

Energy Harvesting and Power Regulation

On-orbit energy harvesting is performed by a modular maximum power-point tracking (MPPT) circuit supplied by 1.5U solar panels with three Spectrolab XTE-SF space qualified triple junction solar cells on each. A total of 8 solar panels (24 cells) are used per spacecraft with the solar output of each panel in parallel. The MPPT design, based on the Analog Devices LT8491, is a high-efficiency buck-boost solar charging solution that is rated up to 600 W.

By implementing a modular mezzanine-style approach, these modules, shown in Fig. 6, can be added to any of the X or Y faces and operated in parallel for reduced risk of single-point subsystem failures. Although the LT8491 is a consumer device, Allen et al. found no destructive SEE or SEL with an LET of 42.2 MeV-cm2/mg at 85C [14]. The Vishay Si7106DN N-channel power MOSFETs were used in the switching regulator design for their SEE and TID radiation performance [15].

Figure 6: MPPT module based on the Analog Devices LT8491.

Spacecraft power regulation relies on the PyCubed on-board DC-DC converter (part number: TPS54226PWPR) to efficiently regulate the 2S3P (8.4 V max) battery voltage to provide 3.3 V necessary to power various spacecraft subsystems. The decision to use the TPS542XX family of DC-DC converters from Texas Instruments was based on its radiation performance, regulator efficiency, and configurable output voltage. Cochran et al. reported a TID tolerance of 15 to 20 krad [16], and Allen et al. reported no destructive SEL events occurring on devices biased at 10V or less and under a variety of temperature conditions [14] for this device.

Communication, Sensing, and Navigation

Cross-link communication and two-way time-of-flight ranging are both performed by Semtech SX1280 (S-band) LoRa radio modules. These radios have a transmit power of 0.5 W and utilize the unique LoRa chirp spread-spectrum modulation [10]. Due to their large bandwidth, LoRa chirp signals are ideal for performing accurate range measurements between two radios. While this sort of time-of-flight ranging has been implemented in software with previous LoRa radios [10], the SX1280 is the first LoRa module to implement ranging capabilities at the hardware level. As a result, sub-meter range accuracy is achievable with careful calibration [10]. At a cost of only a few dollars, the SX1280 provides a very low-cost navigation solution for CubeSats.

In addition to the S-band SX1280 radio, the PY4 spacecraft also carry a UHF LoRa radio (Semtech SX1276) for communication with ground stations. This radio module has a maximum output power of 1 W and is optimized for robust communication at low data rates for telemetry and command. A high-data-rate mode for this radio is also implemented in flight software for downlinking larger volumes of experiment data.

To provide ground-truth navigation data to validate LoRa range measurements, and to enable absolute orbit determination, the PY4 spacecraft are also equipped with a NovAtel OEM719 GPS receiver connected to an active patch antenna located on the +Z face.

In addition to radio measurement hardware, each PY4 spacecraft is also equipped with an IMU (Bosch BMX160), which includes a MEMS gyroscope and magnetometer for use in attitude determination and control algorithms. The spacecraft also have individually addressable sun sensors (Texas Instruments OPT3001) and H-bridge controllers (Texas Instruments DRV8830) on all six faces to aid in attitude determination and to drive magnetic torque coils to perform sun pointing.

Finally, each PY4 spacecraft is also equipped with a custom-built radiation dosimeter to collect total ionizing dose (TID) information. These sensors work by measuring the threshold voltage (V_{TH}) in a commercial P-channel MOSFET (Vardis VT101) designed for dosimetry with known TID response characteristics. A custom direct-redout circuit was developed to make these measurements [12].

Computing

The PY4 spacecraft rely on a Microchip ATSAMD51 ARM Cortex M4F microcontroller as the primary flight computer. This 32-bit microcontroller is clocked at 120 MHz, has 192 kB of RAM and 512 kB of on-board flash memory, and has a hardware floating-point unit. External magnetic random access (MRAM) non-volatile flash memory (part number: MR25H40MDF) is used to store flight software in the form of plain-text Python source-code files and an external SD card (part number: SDSDQED-008G-XI) is used for data storage.

The ATSAMD51 microcontroller utilizes common serial communication protocols such as Inter-Integrated Circuit (I2C) and Serial Peripheral Interface (SPI) to interface with the various on-board sensors, radios, and data storage devices. Including power monitors, sun sensors, and H-bridge drivers, a single PY4 spacecraft can have up to 30 devices on a single I2C bus. Given the inherent single-point failure mode of these serial protocols, an autonomous fault isolation circuit was developed [12]. By automatically isolating failed devices, the integrity of the bus is preserved without requiring additional signals or processing overhead from the host controller.

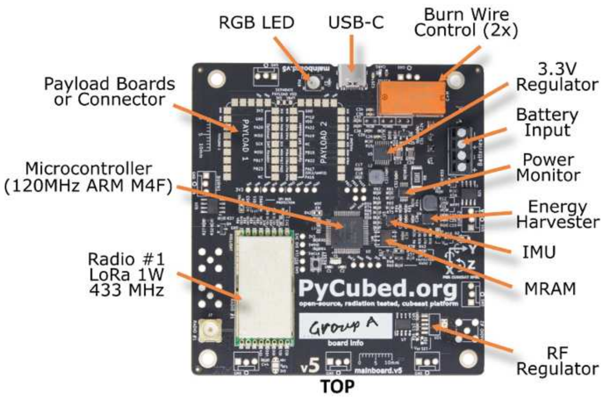

Figure 7: PyCubed mainboard. This single PC-104 board provides computing, power regulation, radio communication, GPS, and IMU capabilities. Python-based software decreases development effort and improves reliability.

Flight Software

All high-level flight software executed on the PY4 spacecraft is implemented in Python. As discussed in [8], the Micropython and CircuitPython real-time Python interpreters provide a robust CubeSat software architecture that is easier to learn, faster to program, and simpler to troubleshoot and debug than traditional embedded C and C++ approaches. The inherent compartmentalization, memory safety, and robust fault tolerance of Python's virtual machine enables the rapid software development necessary for the PY4 mission.

ATTITUDE CONTROL

PY4 implements a novel magnetorquer-only sun-pointing algorithm to achieve safe, stable sun pointing control with a minimum of sensor and actuator hardware. This algorithm seamlessly integrates spin-axis stabilization and sun-pointing within a unified Lyapunov-based controller framework that provides strong stability and convergence guarantees despite the inherent underactuation of magnetorquer-based control methods. Its simplicity and low hardware cost make this control method particularly suitable as a safe-mode controller to put a spacecraft in a stable sun-pointing attitude to maintain positive power generation.

Algorithm 1 summarizes the controller's operation, where h is the satellite's angular momentum, s is the inertially fixed Sun-vector, B is the Earth's magnetic field expressed in the satellite body frame (as measured by the onboard magnetometer), ω is the satellite's angular velocity expressed in the body frame (as measured by the onboard gyroscope), ω_b is an estimate of the gyro bias, h_{tgt} is the desired target angular momentum, I is the inertia matrix of the satellite, u is the control command, u_{max} is the maximum magnetic dipole that can be generated by the magnetorquers, and tol_{FS} and tol_{SP} are convergence tolerances for spin stabilization and sun pointing, respectively.

Algorithm 1 Lyapunov-based Sun-pointing hybrid controller

Data :$s(t), B(t), \omega(t), h_{tgt}, I$
Output :u
$h = I \cdot (\omega + \omega_b)$
if $\|I_{Max} - \frac{h}{\|h_{tgt}\|} > tol_{FS}\|$ **then**
  $u = \hat{B}\left(I_{Max} - \frac{h}{\|h_{tgt}\|}\right)$
else if $\|s - \frac{h}{\|h\|}\| > tol_{SP}$ **then**
  $u = \hat{B}\left(s - \frac{h}{\|h\|}\right)$
else
  $u = [0 \quad 0 \quad 0]^T$
end if
$u = u_{max} \cdot \frac{u}{\|u\|}$

RELATIVE NAVIGATION

The PY4 spacecraft use a combination of S-band inter-satellite ranging and GPS to perform full orbit determination. This section will use the nomenclature "anchor" to describe a spacecraft that has access to GPS measurements and "chaser" to describe a spacecraft that has access only to range measurements to the anchor (and possibly other chaser spacecraft as well). This assignment is arbitrary since all PY4 spacecraft are identical and can serve either role.

Since range measurements between two spacecraft are scalar distances, reconstructing the full relative positions of the chaser spacecraft is impossible given only a single measurement. To solve the orbit-determination problem for a chaser spacecraft, a batch state-estimation problem is posed to reconstruct the position and velocity of the chaser by combining GPS measurements from the anchor with ranging measurements.

Recursive Bayesian state-estimation techniques like the Kalman Filter and its many extensions, including the Extended Kalman Filter are widely used methods for recovering full state estimates given limited sensor measurements [17]. However, in situations where the dynamics and sensor measurements are highly nonlinear, a batch state estimation approach can perform better. Batch methods formulate the state-estimation problem as an optimization problem that recovers the maximum a-posteriori (MAP) estimate of the state history given a history of measurements.

To formulate the chaser orbit determination problem in this framework, we first define the dynamics function for the spacecraft,

$$x_{k+1} = f(x_k) + w_k ,$$

where x is the spacecraft state vector (position and velocity), k is a discrete time step, f is a dynamics function that includes a high-order gravity model and atmospheric drag effects, and w is additive noise assumed to be drawn from a multivariate normal distribution with zero mean and covariance Q.

Range measurements between chaser and anchor spacecraft are similarly modeled by a measurement function,

$$y_k = g(x_k) + v_k ,$$

where y_k is a single measurement taken at time k, g is a function mapping full states into range measurements, and v is additive noise assumed to be drawn from a normal distribution with zero mean and variance R.

Given a set of measurements $y_{1:N}$, the MAP state estimation problem can be stated as:

$$\min_{x_1,\ldots,x_N} \sum_{k=1}^{N-1} \left(x_{k+1} - f(x_k)\right)^T Q^{-1}\left(x_{k+1} - f(x_k)\right) + \left(y_k - g(x_k)\right)^T R^{-1}(y_k - g(x_k)) ,$$

which can be equivalently restated in the following form:

$$\min_{x_1,\ldots,x_N} \sum_{k=1}^{N-1} \left\| \begin{bmatrix} \sqrt{Q^{-1}}(x_{k+1} - f(x_k)) \\ \sqrt{R^{-1}}(y_k - g(x_k)) \end{bmatrix} \right\|_2^2$$

The problem is now clearly in the form of a nonlinear least-squares problem, which can be solved by many standard algorithms. We utilize the Levenberg-Marquardt method, which is a modification of Newton's method that includes regularization and a line search to guarantee local convergence on nonlinear problems [18].

DRAG-BASED FORMATION CONTROL

As part of a planned extended mission, the PY4 spacecraft will demonstrate a drag-based formation-flying technique developed by several of the authors and described in [19]. Our method builds on ideas pioneered by Planet [2] for deploying their imaging CubeSats into a "string-of-pearls" or "ring" formations. While the Planet method is limited to along-track control, our method is able to achieve both along-track and cross-track separation between spacecraft using only drag modulation.

Achieving cross-track separation relies on the so-called "J2 effect," also known as nodal precession. Due to the oblateness of the Earth, inclined orbits tend to precess, or rotate about the Earth's polar axis (their right ascension changes over time). The rate of this precession is altitude dependent, and increases as altitude decreases. We take advantage of this phenomena by using drag to lower one satellites orbit while keeping another in a higher orbit. The lower satellite's precession rate then increases, leading to cross-track separation. When the desired separation is achieved, the higher satellite can be lowered so that the precession rates match again. For more details, we refer the interested reader to [19].

INITIAL ON-ORBIT RESULTS

Both sun-pointing and range-based relative navigation experiments have been successfully performed on multiple PY4 spacecraft. This section presents representative data collected during two such experiments.

Sun Pointing

The magnetorquer-only sun-pointing controller was run successfully multiple times on multiple PY4 spacecraft. A representative plot of 20 minutes of spacecraft gyroscope data is shown in Fig. 8. As the plot demonstrates, the spacecraft is able to transition from a slow tumble to a stable major-axis spin of 20 deg/s with very small residual nutation or wobble. Placing the spacecraft in a major-axis or "flat" spin ensures passive stability once the controller is turned off.

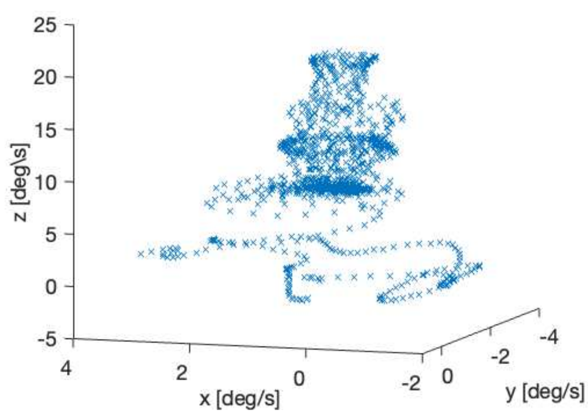

Figure 8: Scatter plot of gyroscope data collected during a 20-minute run of the sun-pointing controller. The spacecraft transitions from a slow tumble to a 20 deg/s spin about its major axis of inertia with very small residual nutation.

A representative plot of the sun unit-vector expressed in the body frame as measured by the onboard sun sensors is shown in Fig. 9. As can be seen in the plot, the sun vector (green) converges to within 10 deg of the desired direction (blue circle), at which point the controller is turned off and the spacecraft remains passively stable.

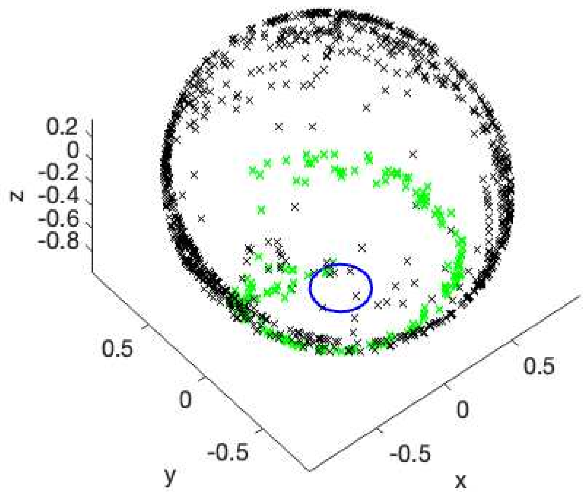

Figure 9: Scatter plot of sun-vector data collected during a run of the sun-pointing controller. Black data points represent tumbling before the controller is activated. Green dots show convergence to the desired sun-pointing attitude once the controller is activated.

Range-Based Relative Navigation

Inter-satellite range data was collected between all pairs of PY4 spacecraft during the first few days of the mission, along with GPS position and velocity measurements. This section presents preliminary analysis for one dataset collected over a 64-minute period of time between PY4-B and PY4-C.

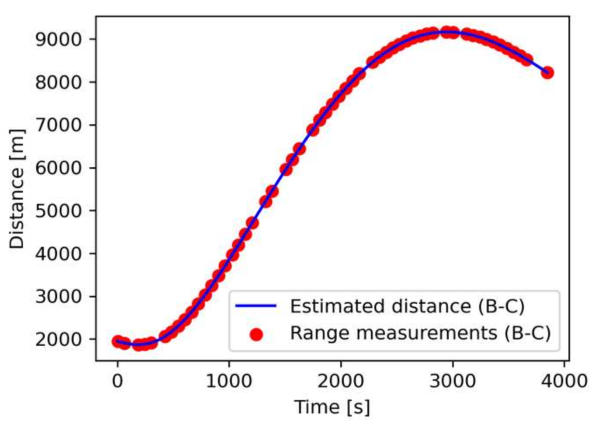

Figure 10: Estimated inter-satellite range (blue) and individual range measurements (red) showing close agreement.

Since individual GPS position measurements are only accurate to tens of meters, the full GPS dataset was smoothed using a high-fidelity orbital-dynamics model to build a "ground-truth" reference orbit. Range data between satellites B and C was then used to estimate the relative orbital state vector of satellite C, with satellite B as the anchor node.

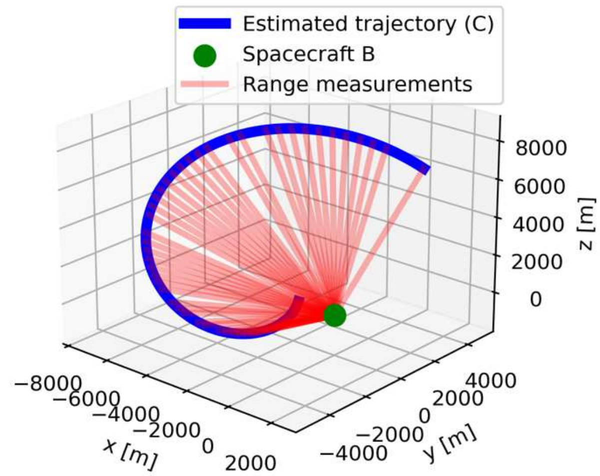

Figure 11: Estimated 3D spacecraft trajectory (blue) and individual range measurements (red). An RMS error of 4.2 m was achieved for 3D relative positions.

Figure 10 shows the estimated inter-satellite range (blue) as well as the individual measurements (red), demonstrating an extremely close fit to the data. Figure 11

shows the full estimated trajectory of spacecraft C relative to spacecraft B (blue) as well as the individual range measurements (red). The RMS error in the full 3D relative positions was 4.2 m, which is well below the mission requirement of 100 m.

CONCLUSIONS

PY4 has made significant progress toward the goal of creating fully autonomous swarms of low-cost small satellites. Building on the lessons learned from the V-R3x mission, PY4 has successfully demonstrated high-speed mesh networking between satellites, over-the-air software updates, magnetorquer-only sun pointing, precise inter-satellite ranging, and orbit determination of a chaser spacecraft based on inter-satellite ranging to an anchor spacecraft with a known orbit.

While the primary mission objectives of PY4 have been achieved, there is still much to do in both an extended PY4 mission and future follow-on missions: We hope to build on the success of PY4's range-based orbit determination and magnetorquer-based attitude control capabilities to demonstrate formation flying using drag modulation. This combination of capabilities paves the way for small satellites that can control their attitude and formation fly without costly and failure-prone reaction wheels or propulsion systems.

ACKNOWLEDGMENTS

This work was supported by NASA's Space Technology Mission Directorate (STMD) Small Satellite Technology Program (SSTP) under NASA Grant Number 80NSSC21K0446.

The authors would like to thank Watson Attai (NASA ARC) for his help building, testing, and operating the spacecraft, as well as the global community of amateur radio operators and the TinyGS network of ground stations for the tens of thousands of PY4 beacons collected worldwide. A special thanks is extended to three HAMs whose contributions were crucial to the mission's success: Stefan (OE6ISP), Scott Chapman (K4KDR), and Bob Mattaliano (N6RFM).

REFERENCES

[1] C. Foster, H. Hallam, and J. Mason, "Orbit Determination and Differential-drag Control of Planet Labs Cubesat Constellations." arXiv, Sep. 10, 2015. Accessed: Jun. 10, 2024. [Online]. Available: http://arxiv.org/abs/1509.03270

[2] C. Foster *et al.*, "Constellation Phasing with Differential Drag on Planet Labs Satellites," *Journal of Spacecraft and Rockets*, vol. 55, no. 2, pp. 473–483, Mar. 2018, doi: 10.2514/1.A33927.

[3] B. Lucia, B. Denby, Z. Manchester, H. Desai, E. Ruppel, and A. Colin, "Computational Nanosatellite Constellations: Opportunities and Challenges," *GetMobile: Mobile Comp. and Comm.*, vol. 25, no. 1, pp. 16–23, Jun. 2021, doi: 10.1145/3471440.3471446.

[4] S. Engelen, C. J. M. Verhoeven, and M. J. Bentum, "Olfar, A Radio Telescope Based on Nano-Satellites in Moon Orbit," *Small Satellite Conference*, Aug. 2010.

[5] S. Wu, W. Chen, Y. Zhang, W. Baan, and T. An, "SULFRO: a Swarm of Nano-/Micro-Satellite at SE L2 for Space Ultra-Low Frequency Radio Observatory," *Small Satellite Conference*, Aug. 2014.

[6] F. Alibay, J. C. Kasper, T. J. W. Lazio, and T. Neilsen, "Sun radio interferometer space experiment (SunRISE): Tracking particle acceleration and transport in the inner heliosphere," in *2017 IEEE Aerospace Conference*, Big Sky, MT, USA: IEEE, Mar. 2017, pp. 1–15. doi: 10.1109/AERO.2017.7943789.

[7] K. G. Klein *et al.*, "HelioSwarm: A Multipoint, Multiscale Mission to Characterize Turbulence." arXiv, Jun. 10, 2023. Accessed: Jun. 10, 2024. [Online]. Available: http://arxiv.org/abs/2306.06537

[8] M. Holliday, A. Ramirez, C. Settle, T. Tatum, D. Senesky, and Z. Manchester, "PyCubed: An Open-Source, Radiation-Tested CubeSat Platform Programmable Entirely in Python," *Small Satellite Conference*, Aug. 2019.

[9] M. Holliday, K. Tracy, Z. Manchester, and A. Nguyen, "The V-R3x Mission: Towards Autonomous Networking and Navigation for CubeSat Swarms," in *4S Symposium*, Vilamoura, Portugal, May 2022.

[10] T. Janssen, N. BniLam, M. Aernouts, R. Berkvens, and M. Weyn, "LoRa 2.4 GHz Communication Link and Range," *Sensors*, vol. 20, no. 16, p. 4366, Aug. 2020, doi: 10.3390/s20164366.

[11] T. Qin, D. Qiao, and M. Macdonald, "Relative Orbit Determination Using Only Intersatellite Range Measurements," *Journal of Guidance, Control, and Dynamics*, vol. 42, no. 3, pp. 703–710, Mar. 2019, doi: 10.2514/1.G003819.

[12] M. Holliday, Z. Manchester, and D. G. Senesky, "On-Orbit Implementation of Discrete Isolation Schemes for Improved Reliability of Serial Communication Buses," *IEEE Trans. Aerosp. Electron. Syst.*, vol. 58, no. 4, pp. 2973–2982, Aug. 2022, doi: 10.1109/TAES.2022.3142713.

[13] Z. Manchester, M. Peck, and A. Filo, "KickSat: A Crowd-Funded Mission to Demonstrate the World's Smallest Spacecraft," *Small Satellite Conference*, Aug. 2013.

[14] G. R. Allen *et al.*, "2017 Compendium of Recent Test Results of Single Event Effects Conducted by the Jet Propulsion Laboratory's Radiation Effects Group," in *2017 IEEE Radiation Effects Data Workshop (REDW)*, New Orleans, LA: IEEE, Jul. 2017, pp. 1–9. doi: 10.1109/NSREC.2017.8115429.

[15] T. Fairbanks, H. Quinn, J. Tripp, J. Michel, A. Warniment, and N. Dallmann, "Compendium of TID, Neutron, Proton and Heavy Ion Testing of Satellite Electronics for Los Alamos National Laboratory," in *2013 IEEE Radiation Effects Data Workshop (REDW)*, Jul. 2013, pp. 1–6. doi: 10.1109/REDW.2013.6658191.

[16] D. J. Cochran *et al.*, "Total Ionizing Dose and Displacement Damage Compendium of Candidate Spacecraft Electronics for NASA," in *2009 IEEE Radiation Effects Data Workshop*, Jul. 2009, pp. 25–31. doi: 10.1109/REDW.2009.5336318.

[17] S. Thrun, W. Burgard, and D. Fox, *Probabilistic robotics*. in Intelligent robotics and autonomous agents. Cambridge, Mass: MIT Press, 2005.

[18] J. Nocedal and S. J. Wright, *Numerical optimization*, 2nd ed. in Springer series in operations research and financial engineering. New York: Springer, 2006.

[19] G. Falcone, J. B. Willis, and Z. Manchester, "Propulsion-Free Cross-Track Control of a LEO Small-Satellite Constellation with Differential Drag," in *2023 62nd IEEE Conference on Decision and Control (CDC)*, Singapore, Singapore: IEEE, Dec. 2023, pp. 8738–8744. doi: 10.1109/CDC49753.2023.1038414